Journal of Sound and Vibration 326 (2009) 633–646

Contents lists available at ScienceDirect

Journal of Sound and Vibration

journal homepage: www.elsevier.com/locate/jsvi

# Free vibration analysis of ring-stiffened cylindrical shells using wave propagation approach

Lin Gan *, Xuebin Li, Zheng Zhang

*Wuhan 2nd Ship Design and Research Institute, Wuhan, Hubei Province 430064, PR China*

ARTICLE INFO

*Article history:*
Received 23 August 2008
Received in revised form
26 February 2009
Accepted 1 May 2009
Handling Editor: J. Lam
Available online 29 May 2009

ABSTRACT

The wave propagation approach is used to analyze the free vibration of ring-stiffened cylindrical shell under initial hydrostatic pressure, based on Flügge classical thin shell theory and orthotropic method in this paper. The results obtained are compared with those available in other literature. It has been proved that, free vibration analysis using wave propagation approach with shear diaphragm–shear diaphragm (SD–SD) boundary conditions is absolutely equal to the traditional method. To evaluate the validity and accuracy of the wave propagation approach, an exact solution for arbitrary boundary conditions is also proposed in this paper. The comparisons between these two approaches are carried out for clamped–clamped (C–C) and clamped–shear diaphragm (C–SD) boundary conditions. The results show that wave propagation has high accuracy for long shell and large circumferential numbers.



## 1. Introduction

Circular cylindrical shells are widely used in many structural applications such as airplanes, marine crafts and construction buildings. Usually cylinders are stiffened by rings or stringers to increase the stiffness and strength, reduce the weight of structure to be designed. Many investigations have been developed to analyze the vibration behavior of thin cylindrical shells, e.g. Refs. [1–5]. These methods range from energy methods based on the Rayleigh–Ritz procedure to analytical methods in which, respectively, closed form solutions of the governing equations and iterative solution approaches were used. Most of the researchers take active interest in the vibration analysis of circular cylindrical shells with shear diaphragm–shear diaphragm (SD–SD) boundary conditions, as the solution to the equations of motion has a simple form of trigonometric functions which can satisfy the SD–SD boundary conditions exactly. For arbitrary boundary conditions, many authors [6–10] have chosen exponential functions for the modal displacement along the axial direction, substituted them into the equations of motion and then enforced the eighth-order frequency determinants which are coupled together.

The wave propagation approach, which is a simple, non-iterative and effective method, has been used for vibration analysis of thin cylindrical shells with different boundary conditions. Wang and Lai [11] used this approach to study the vibration behavior of finite length circular cylindrical shells based on Love's shell theory and gave an approximate method for calculating the natural frequencies of finite length circular cylindrical shells with different boundary conditions without simplifying the exact equations of motion. Zhang et al. [12] studied the vibration characteristics of thin cylindrical shells using wave propagation approach based on Love's shell theory, calculated the frequencies and compared the results by the

* Corresponding author.
*E-mail address:* glrain002@163.com (L. Gan).

0022-460X/$ - see front matter © 2009 Elsevier Ltd. All rights reserved.
doi:10.1016/j.jsv.2009.05.001

**Nomenclature**

| | |
|---|---|
| $A_2$ | sectional area of stiffener |
| $b_r$ | width of the rectangular stiffener |
| $B$ | stretching stiffness of the shell, $B=\frac{Eh}{1-\upsilon^2}$ |
| $d_2$ | stiffener spacing |
| $D$ | bending stiffness of the shell, $D=\frac{Eh^3}{12(1-\upsilon^2)}$ |
| $e_2$ | eccentricity of the centroid of the ring stiffener section, $e_2=\frac{1}{2}(h+h_r)$ |
| $E$ | modulus of Young's elasticity |
| $G$ | shear modulus |
| $h$ | thickness of the shell |
| $\bar{h}$ | $h+\frac{A_2}{d_2}$ |
| $h_r$ | height of the rectangular stiffener |
| i | $\sqrt{-1}$ |
| $I_0$ | sectional moment of inertia of the stiffener about the centroid of the stiffener |
| $I_2$ | sectional moment of inertia of the stiffener about the middle surface of the shell |
| $J_2$ | torsion constant of stiffener cross-section |
| $k$ | $\frac{h^2}{12R^2}$ |
| $k_m$ | wavenumber in the axial direction (wave propagation) |
| $L$ | length of the shell |
| $m$ | number of axial half-wave |
| $n$ | number of circumferential waves |
| $Q$ | external hydrostatic pressure |
| $R$ | radius of the shell |
| $t$ | time |
| $x, \theta, z$ | cylindrical coordinates (Fig. 1) |
| $u, v, w$ | components of the displacement in the $x$, $\theta$ and $z$ directions |
| $\lambda$ | axial factor |
| $\upsilon$ | Poisson's ratio |
| $\rho$ | mass density |
| $\omega$ | circular frequency of shell |

wave propagation method and numerical finite element method. Zhang et al. have also extended this approach to coupled vibration of fluid-filled shells [13], submerged shells [14] and cross-ply laminated composite shells [15]. Li [16] studied free vibration of a circular cylindrical shell *in vacuo* using wave propagation approach based on Flügge theory, the result obtained are compared with exact solution to evaluate the accuracy and validity of this approach and studied the dispersion characteristics of circular cylindrical shell. Xu et al. [17–20] studied the power flow propagating in fluid-filled shells using the wave propagation approach.

In this paper, the free vibration analysis of a ring-stiffened cylindrical shell under initial hydrostatic pressure is investigated using wave propagation approach based on Flügge classical thin shell theory. The effects of ring stiffeners are "smeared out" over the surface of the shell, the stiffened shell can be modeled as an equivalent uniform orthotropic shell. In the present method, the axial mode function of ring-stiffened cylindrical shell is approximately obtained from the beam function with the same boundary conditions. The error may be introduced due to neglecting the coupling effect between the axial and circumferential modes by using the beam function. In order to evaluate the validity and accuracy of the wave propagation approach, an exact solution for free vibration of ring-stiffened cylindrical shell is also given in this paper. The comparisons of these two methods for natural frequencies are carried out for ring-stiffened cylindrical shells with shear diaphragm–shear diaphragm, clamped–clamped (C–C) and clamped–shear diaphragm (C–SD) boundary conditions. The results show that wave propagation has high accuracy for long shell and SD–SD boundary conditions.

## 2. Equations of motion of ring-stiffened cylindrical shell

The ring-stiffened cylindrical shell under consideration has constant thickness $h$, radius $R$ and length $L$. The reference surface is taken at the middle surface of the shell where an orthogonal coordinate system $(x, \theta, z)$ is fixed. The $x$ coordinate is taken in the axial direction of the shell, where $\theta$ and $z$ are, respectively, in the circumferential and radial directions of the shell as shown in Fig. 1. The displacements of the shell are defined by $u$, $v$ and $w$ in the $x$, $\theta$ and $z$ directions, respectively. The ring stiffeners and the shell consist of the same linear elastic material.

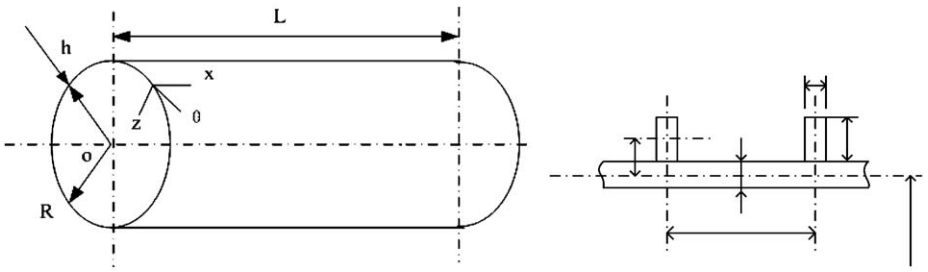


**Fig. 1.** Ring-stiffened cylindrical shell and stiffener.

The equations of motion for cylindrical shell under hydrostatic pressure can be written using Flügge theory as

$$\frac{\partial N_x}{\partial x}+\frac{\partial N_{\theta x}}{R\partial\theta}-Q\left(\frac{\partial^2 u}{R\partial\theta^2}+\frac{\partial w}{\partial x}\right)-\frac{RQ}{2}\frac{\partial^2 u}{\partial x^2}=\rho\bar{h}\frac{\partial^2 u}{\partial t^2}$$

$$\frac{\partial N_{x\theta}}{\partial x}+\frac{\partial N_\theta}{R\partial\theta}-\left(\frac{\partial M_\theta}{R^2\partial\theta}+\frac{\partial M_{x\theta}}{R\partial x}\right)-Q\left(\frac{\partial^2 v}{R\partial\theta^2}-\frac{\partial w}{R\partial\theta}\right)-\frac{RQ}{2}\frac{\partial^2 v}{\partial x^2}=\rho\bar{h}\frac{\partial^2 v}{\partial t^2}$$

$$\frac{\partial^2 M_x}{\partial x^2}+\frac{\partial^2 M_{x\theta}}{R\partial x\partial\theta}+\frac{\partial^2 M_{\theta x}}{R\partial\theta\partial x}+\frac{\partial^2 M_\theta}{R^2\partial\theta^2}+\frac{N_\theta}{R}+Q\left(\frac{\partial u}{\partial x}-\frac{\partial v}{R\partial\theta}-\frac{\partial^2 w}{R\partial\theta^2}\right)-\frac{RQ}{2}\frac{\partial^2 w}{\partial x^2}=\rho\bar{h}\frac{\partial^2 w}{\partial t^2} \tag{1}$$

The forces and moments are given in Appendix A. Letting the $Q=0$ in Eq. (1), the equations of motion *in vacuo* can be obtained.

The displacements of the shell can be expressed in the form of wave propagation as follows:

$$u=U_m\cos n\theta e^{i\omega t-ik_m x}$$

$$v=V_m\sin n\theta e^{i\omega t-ik_m x}$$

$$w=W_m\cos n\theta e^{i\omega t-ik_m x} \tag{2}$$

where $U_m$, $V_m$ and $W_m$ are the wave amplitudes of the displacement in the $x$, $\theta$ and $z$ directions, respectively, $k_m$ and $n$ are axial wavenumber and circumferential modal parameter, $\omega$ is the circular driving frequency.

Substituting Eq. (2) into Eq. (1), it can be written as

$$\begin{bmatrix}\gamma\omega^2-K_{11} & K_{12}i & K_{13}i\\ K_{21}i & \gamma\omega^2-K_{22} & K_{23}\\ K_{31}i & K_{32} & \gamma\omega^2-K_{33}\end{bmatrix}\begin{Bmatrix}U_m\\ V_m\\ W_m\end{Bmatrix}=\{0\} \tag{3}$$

where $K_{ij}$ $(i,j=1,2,3)$ are the coefficients, which are listed in Appendix B; $\gamma=\bar{h}\rho R^2/B$. For the non-trivial solutions, one set the determinant of the characteristic matrix in Eq. (3) to zero

$$\begin{vmatrix}\gamma\omega^2-K_{11} & K_{12}i & K_{13}i\\ K_{21}i & \gamma\omega^2-K_{22} & K_{23}\\ K_{31}i & K_{32} & \gamma\omega^2-K_{33}\end{vmatrix}=0,\quad j,k=1,2,3 \tag{4}$$

Expansion of the determinant of above equation provides the system characteristic equation

$$f(k_m,\omega)=0 \tag{5}$$

where $f(k_m,\ \omega)$ is polynomial function. Eq. (5) is used to calculate the natural frequency of the finite ring-stiffened cylindrical shell. In order to calculate the frequencies, only the wavenumber $k_m$ in the axial direction is needed to determine. The right wavenumber $k_m$ must be chosen to satisfy the boundary conditions at the two ends of the shell. In this analysis the wavenumber in the axial direction of shell is approximately obtained by studying the vibration of a similar beam of the same boundary conditions. Eq. (5) can be written as

$$\omega^6+a_1\omega^4+a_2\omega^2+a_3=0 \tag{6}$$

where $a_i$ $(i=1,\ 2,\ 3)$ are the coefficients of Eq. (6), which are listed in Appendix C. Solving this equation, one can obtain three roots, the lowest root represents the flexural vibration, and the other two are in-plane vibrations.

The beam's wavenumber is used as the axial wavenumber of shell in this method, the error may be introduced due to neglecting the coupling effect between the axial and circumferential modes. In order to evaluate the validity and accuracy of the wave propagation approach, an exact solution for free vibration of the ring-stiffened cylindrical shell is presented here. The displacements of shell can be written in the general form

$$u=U_0e^{\lambda x}\cos n\theta\cos\omega t$$

$$v=V_0e^{\lambda x}\sin n\theta\cos\omega t$$

$$w=W_0e^{\lambda x}\cos n\theta\cos\omega t \tag{7}$$

where the axial factor $\lambda$ is a complex number.

Substitution of Eq. (7) into the equations of motion leads to an eight-order characteristic equation for $\lambda$

$$g_8\lambda^8+g_6\lambda^6+g_4\lambda^4+g_2\lambda^2+g_0=0 \tag{8}$$

where $g_i$ ($i = 0, 2, 4, 6, 8$) are real coefficients, which are listed in Appendix D. For the usual range of shell and stiffener parameters and $n \geq 1$, Eq. (8) has eight roots as following:

$$\lambda = \pm\lambda_1, \quad \pm\lambda_2 \mathrm{i}, \quad \pm(\lambda_3 \pm \lambda_4 \mathrm{i}) \tag{9}$$

where $\lambda_i$ ($i = 1, 2, 3, 4$) are real, positive numbers. The axial and circumferential modal coefficients can be written as

$$\alpha_i = \frac{U_{0i}}{W_{0i}}, \quad \beta_i = \frac{V_{0i}}{W_{0i}}, \quad i = 1, 2, 3, \ldots, 8 \tag{10}$$

These coefficients are calculated for these eight roots. Then, the displacements of shell can be rewritten as [6]

$$w = \begin{bmatrix} C_1 \mathrm{e}^{\lambda_1 x} + C_2 \mathrm{e}^{-\lambda_1 x} + C_3 \cos \lambda_2 x + C_4 \sin \lambda_2 x + C_5 \mathrm{e}^{\lambda_3 x} \cos \lambda_4 x + C_6 \mathrm{e}^{\lambda_3 x} \sin \lambda_4 x \\ + C_7 \mathrm{e}^{-\lambda_3 x} \cos \lambda_4 x + C_8 \mathrm{e}^{-\lambda_3 x} \sin \lambda_4 x \end{bmatrix} \cos n\theta \cos \omega t \tag{11}$$

where $C_i$ ($i = 1, 2, \ldots, 8$) are real independent constants, while $u$ and $v$ have the similar form of expressions which involve combinations of the constants $C_i$ and the real and imaginary parts of $\alpha_i$ and $\beta_i$.

At each end of the shell, four boundary conditions must be specified, these constraints consist of all combinations of the following:

$$u = 0 \quad \text{or} \quad N_x = 0$$

$$v = 0 \quad \text{or} \quad R_x = N_{x\theta} - \frac{1}{R} M_{x\theta} = 0$$

$$w = 0 \quad \text{or} \quad S_x = \frac{\partial M_x}{\partial x} + \frac{1}{R} \frac{\partial M_{\theta x}}{\partial \theta} + \frac{1}{R} \frac{\partial M_{x\theta}}{\partial \theta} = 0$$

$$\frac{\partial w}{\partial x} = 0 \quad \text{or} \quad M_x = 0 \tag{12}$$

Substituting the rewritten displacements into these constraints lead to the system characteristic equation

$$[\mathbf{A}]_{8\times 8} \{C_i\}^{\mathrm{T}} = \{0\}, \quad i = 1, 2, 3, \ldots, 8 \tag{13}$$

where $\mathbf{A}$ is an $8 \times 8$ coefficient matrix whose rows depend on the boundary conditions. Forsberg [6] and Warburton [8] presented different solving methods for this equation.

Three different boundary conditions of the ring-stiffened cylindrical shell are studied in these two approaches: SD–SD, C–C and C–SD boundary conditions. The wavenumber for wave propagation and constraints of boundary conditions of shell are listed in Table 1.

The nondimensional frequency parameter is defined as

$$\Omega^2 = \frac{\rho(1 - \upsilon^2) R^2 \bar{h}}{Eh} \omega^2 \tag{14}$$

## 3. Numerical results and discussion

The wave propagation approach is firstly utilized to calculate the natural frequencies of a ring-stiffened cylindrical shell with SD–SD boundary conditions. The computation model is a ring-stiffened cylindrical shell with evenly spaced and uniform stiffeners eccentricity. An example is given with the geometrical dimensions and material properties of the shell and stiffeners listed in Table 2, there are three kinds of stiffeners with different cross-section heights, $h_{r1} = 0.291 \times 10^{-2}$ m, $h_{r2} = 0.582 \times 10^{-2}$ m and $h_{r3} = 0.582 \times 10^{-2}$ m, respectively. The circular frequencies of free vibration *in vacuo* obtained here are compared with those from other literature in Table 3, where a value of $m = 1$ is used and $n$ are chosen from 2 to 5. The next example for the free vibration *in vacuo* of a ring-stiffened cylindrical shell is also given here. The geometrical dimensions and material properties of shell and stiffener are listed in Table 4, and the comparison of the natural frequencies for this case are carried out with the experimental results and also the analytical results by energy method of

**Table 1**
Wavenumber and boundary conditions.

| Boundary conditions of shell | Wavenumber | Constraints |
|---|---|---|
| Shear diaphragm–shear diaphragm (SD–SD) | $K_m L = m\pi$ | $v = w = N_x = M_x = 0,\ x = 0, L$ |
| Clamped–clamped (C–C) | $K_m L = (2m+1)\pi/2$ | $u = v = w = \frac{\partial w}{\partial x} = 0,\ x = 0, L$ |
| Clamped–shear diaphragm (C–SD) | $K_m L = (4m+1)\pi/4$ | $u = v = w = \frac{\partial w}{\partial x} = 0\ x = 0$<br>$v = w = N_x = M_x = 0,\ x = L$ |

**Table 2**
Geometrical and material properties of a stiffened shell.

| Characteristics | Geometrical dimensions and material properties |
|---|---|
| $R$ (m) | $10.37 \times 10^{-2}$ |
| $h$ (m) | $0.119 \times 10^{-2}$ |
| $L$ (m) | $47.09 \times 10^{-2}$ |
| $h_r$ (m) (three kinds) | $0.291 \times 10^{-2}$, $0.582 \times 10^{-2}$, $0.873 \times 10^{-2}$ |
| $b_r$ (m) | $0.218 \times 10^{-2}$ |
| $d_2$ (m) | $3.14 \times 10^{-2}$ |
| $E$ (GPa) | 2.06 |
| $\rho$ (kg/m$^3$) | 7700 |
| $\upsilon$ | 0.3 |
| Stiffening type | External |

**Table 3**
Comparison of circular frequencies of stiffened shell $\omega$ (rad/s) ($m = 1$)

| $h_r$ (cm) | $n$ | (a) | (b) | (c) | (d) | Present |
|---|---|---|---|---|---|---|
| 0.291 | 2 | 4550 | 4470 | 4314 | 4420 | 4409 |
| | 3 | 3870 | 3655 | 3173 | 3680 | 3674 |
| | 4 | 6550 | 5950 | 4565 | 6000 | 6000 |
| | 5 | 10 000 | 9510 | 7058 | 9620 | 9604 |
| 0.582 | 2 | 4580 | 4450 | 4235 | | 4481 |
| | 3 | 6710 | 6235 | 4615 | | 6492 |
| | 4 | 12 830 | 11 790 | 7982 | | 12 149 |
| | 5 | 20 120 | 19 020 | 12 660 | | 19 694 |
| 0.873 | 2 | 5040 | 4885 | 4378 | | 4954 |
| | 3 | 10 330 | 9500 | 6651 | | 9873 |
| | 4 | 20 200 | 18 010 | 12 154 | | 18 884 |
| | 5 | 31 800 | 25 570 | 19 221 | | 30 606 |

(a) Basdekas and Chi [21].
(b) Galletly [22].
(c) Wah and Hu [23].
(d) Bosor (smeared rings) [24].

**Table 4**
Geometrical and properties of a stiffened shell.

| Characteristics | Geometrical dimensions and material properties |
|---|---|
| $R$ (m) | $4.9759 \times 10^{-2}$ |
| $h$ (m) | $0.1651 \times 10^{-2}$ |
| $L$ (m) | $39.45 \times 10^{-2}$ |
| $h_r$ (m) | $0.5334 \times 10^{-2}$ |
| $b_r$ (m) | $0.3175 \times 10^{-2}$ |
| $d_2$ (m) | $1.9725 \times 10^{-2}$ |
| $E$ (GPa) | 68.95 |
| $\rho$ (Kg/m$^3$) | 2762 |
| $\upsilon$ | 0.3 |
| Stiffening type | External |

other researchers in Table 5. In the comparison, $m = 1$ and 2 are used and $n$ are selected from 1 to 5. As can be seen from the comparisons, good agreement with those in the literature is obtained; the wave propagation approach is convenient and effective for SD–SD boundary conditions.

The shear diaphragm boundary condition, which corresponds to the homogenous end condition of a finite shell of length $L$ given as

$$N_x = w = v = M_x = 0, \quad x = 0, L \tag{15}$$

and often loosely called the simply supported (SS–SS) condition, is the most widely used of the shell boundary conditions. These conditions can be closely approximated in physical application simply by means of rigidly attaching a thin, flat,

**Table 5**
Comparison of natural frequencies of stiffened shell $f$ (Hz).

| $m$ | $n$ | (e) | (f) | Experiment (g) | Present |
|---|---|---|---|---|---|
| 1 | 1 | 1199.58 | 1204 | | 1216 |
| | 2 | 1564.47 | 1587 | 1530 | 1635 |
| | 3 | 4387.59 | 4462 | 4080 | 4578 |
| | 4 | 8377.75 | 8559 | | 8781 |
| | 5 | 13 490.7 | 13 780 | | 14 172 |
| 2 | 1 | 3493.59 | 3498 | | 3536 |
| | 2 | 2113.84 | 2129 | 2040 | 2176 |
| | 3 | 4400.58 | 4437 | 4090 | 4573 |
| | 4 | 8392.63 | 8482 | | 8731 |
| | 5 | 13 508.9 | 13 695 | | 14 119 |
| 3 | 1 | 5839.89 | 5844 | | 5907 |
| | 2 | 3378.17 | 3386 | 3200 | 3430 |
| | 3 | 4595.79 | 4627 | 4520 | 4788 |
| | 4 | 8449.89 | 8438 | 7520 | 8728 |
| | 5 | 13 555.4 | 13 595 | | 14 069 |

(e) Jafari and Bagheri [25].
(f) Mustafa and Ali [26].
(g) Hoppmann [27].

circular cover plate at each end [5]. The plate is highly flexible in the $z$ direction as well as in bending but has a large stiffness in its own plane.

The traditional expressions of displacement which satisfy the SD–SD boundary conditions of shell exactly are given as follows [6]:

$$u = U\cos\frac{m\pi x}{l}\cos n\theta\cos\omega t$$

$$v = V\sin\frac{m\pi x}{l}\sin n\theta\cos\omega t$$

$$w = W\sin\frac{m\pi x}{l}\cos n\theta\cos\omega t \tag{16}$$

where $U$, $V$ and $W$ are the wave amplitudes of the displacement in the $x$, $\theta$ and $z$ directions, respectively, $m$ is number of axial half-wave.

Substituting Eq. (16) into Eq. (1), the equations can be written as

$$\begin{bmatrix} \gamma\omega^2 - K'_{11} & K'_{12} & K'_{13} \\ K'_{21} & \gamma\omega^2 - K'_{22} & K'_{23} \\ K'_{31} & K'_{32} & \gamma\omega^2 - K'_{33} \end{bmatrix} \begin{Bmatrix} U \\ V \\ W \end{Bmatrix} = \{0\} \tag{17}$$

where $K'_{ij}$ $(i, j = 1, 2, 3)$ are the coefficients, which are listed in Appendix E. For the non-trivial solution, the determinant of this set of equations must be zero. A characteristic equation similar to Eq. (6) can be obtained from Eq. (17)

$$\omega^6 + b_1\omega^4 + b_2\omega^2 + b_3 = 0 \tag{18}$$

where $b_i$ $(i = 1, 2, 3)$ are the coefficients of Eq. (18), which are listed in Appendix F.

Substituting the $k_m = m\pi/L$ for SD–SD boundary conditions into Eq. (6), a comparison is carried out between $\{a_1, a_2, a_3\}$ of Eq. (6) and $\{b_1, b_2, b_3\}$ here, it can be found that

$$a_1 = b_1, \quad a_2 = b_2, \quad a_3 = b_3 \tag{19}$$

This result shows that Eqs. (6) and (18) are the same. The reasoning certainly seems to give a mathematical explanation for the conclusion that, for a finite length ring-stiffened cylindrical shell under hydrostatic pressure with SD–SD boundary conditions, the free vibration analysis using wave propagation approach is absolutely equal to the traditional method.

As can be seen from Eq. (5), the axial wavenumber $k_m$ varies as the circumferential number $n$ varies. However, $k_m$ is a constant number in wave propagation approach for the given boundary conditions. This assumption which neglects the coupling effects between the axial and circumferential modes will introduce error certainly. The axial wavenumber of shell is exactly equal to that of a beam only in SD–SD boundary conditions.

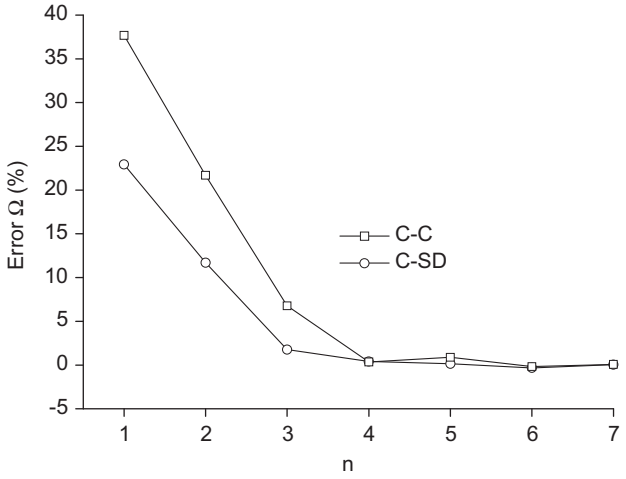


**Fig. 2.** Error curves for frequency *in vacuo* $L/R = 4.54$, $m = 1$, $h_{r1} = 0.291$ cm.

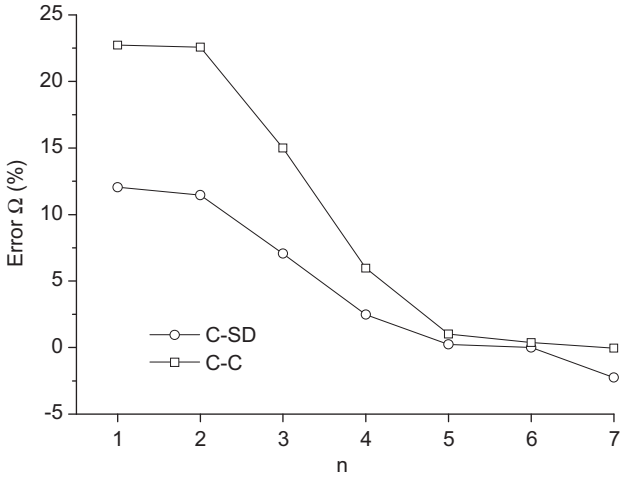


**Fig. 3.** Error curves for frequency *in vacuo* $L/R = 4.54$, $m = 2$, $h_{r1} = 0.291$ cm.

In order to evaluate the accuracy of the wave propagation approach with other boundary conditions, the results from wave propagation are compared with those from exact solution. A relative error parameter is defined as following:

$$\text{Error}_{\Omega} = \frac{\Omega_{\text{wave}} - \Omega_{\text{exact}}}{\Omega_{\text{exact}}} \times 100\% \tag{20}$$

where the subscript wave and exact represent wave propagation method and classical exact method, respectively.

The first example above is used to study the relative error of free vibration frequencies with different shell and stiffeners parameters. The boundary conditions at the two ends of shells are clamped–shear diaphragm and clamped–clamped, respectively. The frequencies comparisons between these two methods are given in Figs. 2–10. The frequencies error can be seen to be more significant at small circumferential number $n$ than at large circumferential number. There is hardly any influence of the boundary conditions at large circumferential numbers. The error for C–C boundary condition is much higher than C–SD boundary condition when $n$ is small. In fact, the coupling effects between the circumferential and axial modes become less significant when the constraints at the end decrease.

The frequencies errors of free vibration of the ring-stiffened cylindrical shell *in vacuo* are shown in Figs. 2 and 3. For $m = 1$, the error is below 10 percent with $n \geq 3$ and the error of the frequencies between these two methods is very small after $n = 4$. While for $m = 2$, the error is below 10 percent after $n = 4$, the error is more significant than that of $m = 1$.

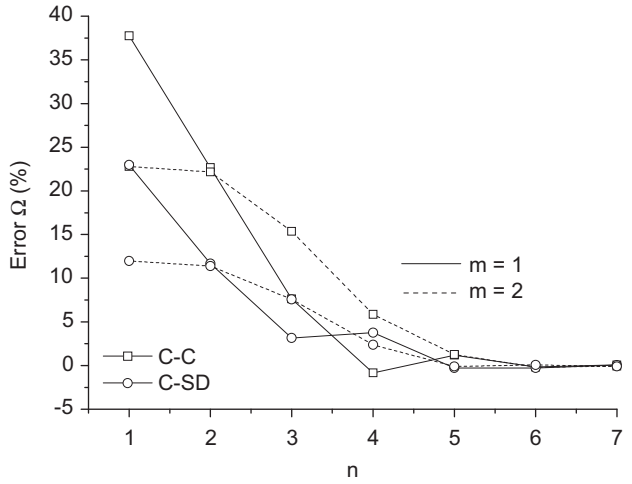


**Fig. 4.** Error curves for frequency ($\bar{Q} = 2 \times 10^{-4}$) $L/R = 4.54$, $h_{r1} = 0.291$ cm.

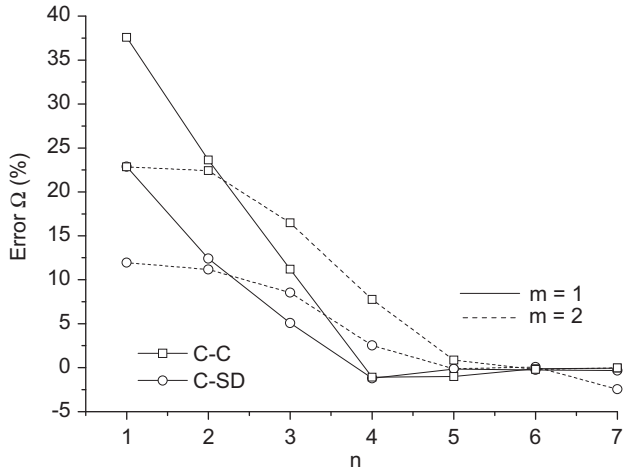


**Fig. 5.** Error curves for frequency ($\bar{Q} = 6 \times 10^{-4}$) $L/R = 4.54$, $h_{r1} = 0.291$ cm.

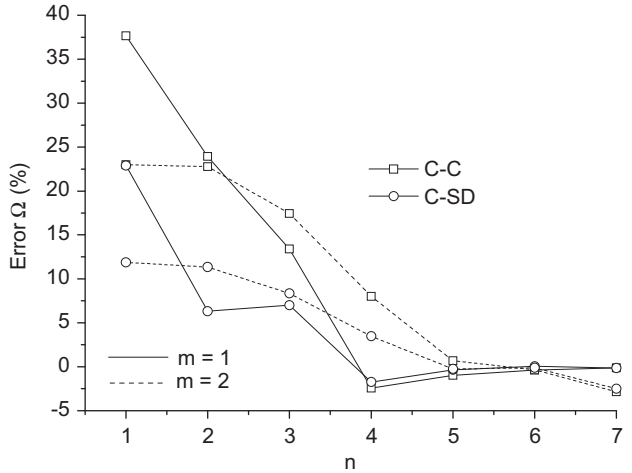


**Fig. 6.** Error curves for frequency ($\bar{Q} = 8 \times 10^{-4}$) $L/R = 4.54$, $h_{r1} = 0.291$ cm.

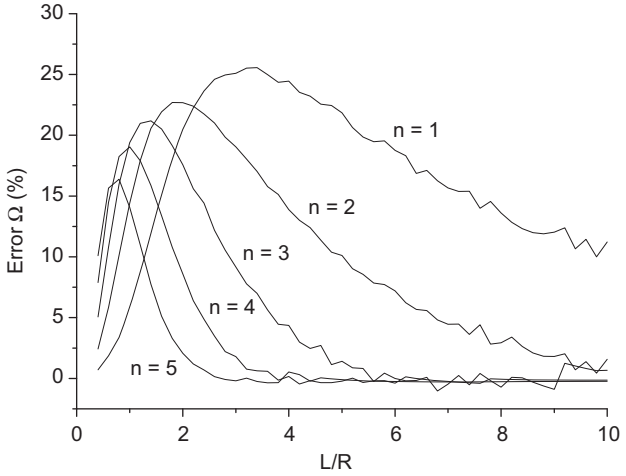


**Fig. 7.** Error curves for frequency of C–SD boundary ($\bar{Q}=0$) $m=1$, $h_{r1}=0.291$ cm.

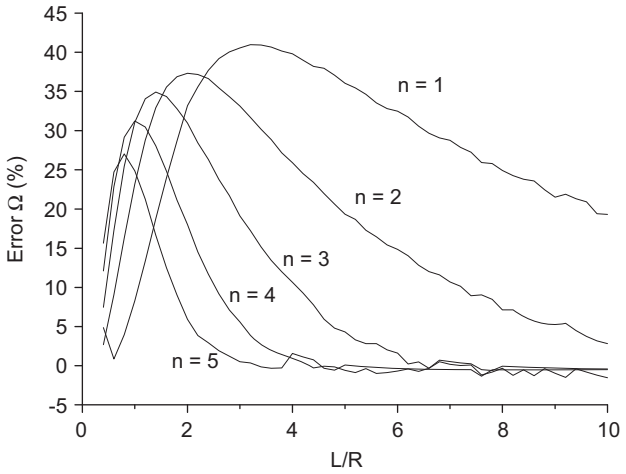


**Fig. 8.** Error curves for frequency of C–C boundary ($\bar{Q}=0$) $m=1$, $h_{r1}=0.291$ cm.

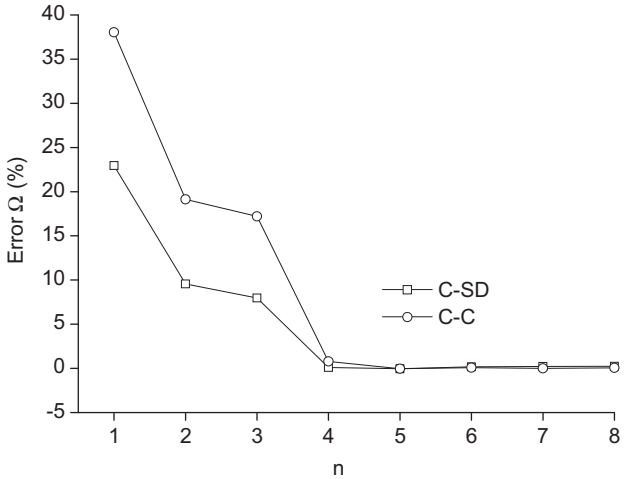


**Fig. 9.** Error curves for frequency $L/R=4.54$, $m=1$, $h_{r2}=0.582$ cm.

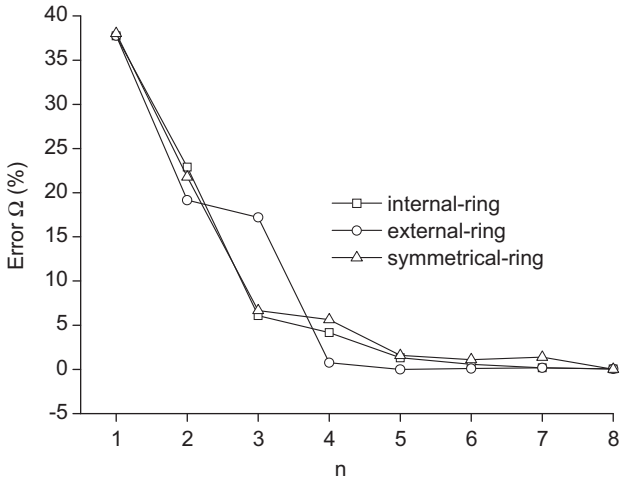


**Fig. 10.** Error curves for frequency of C–C boundary $L/R = 4.54$, $m = 1$, $h_{r2} = 0.582$ cm.

In this paper, hydrostatic pressure is considered as the initial stress. The nondimensional hydrostatic pressure parameter is defined as

$$\bar{Q} = \frac{QR}{Eh}(1 - \upsilon^2) \tag{21}$$

Figs. 4–6 show the frequencies comparisons with the nondimensional initial hydrostatic pressure $\bar{Q} = 2 \times 10^{-4}, 6 \times 10^{-4}, 8 \times 10^{-4}$, respectively. It can be seen that as the $n$ increases, the trend of the error decrease is similar to that *in vacuo*, but slightly slower than it. For certain lower circumferential number $n$, the frequencies error of ring-stiffened cylindrical shell under initial stress is lager than that *in vacuo*.

For short shells, the differences of frequencies between results obtained by the wave propagation method and the exact solution are substantial. The coupling effects between axial and circumferential modes are more important for short shells than that of long shells. Figs. 7 and 8 show the frequencies error varies with the ratio of $L/R$ for clamped–shear diaphragm, clamped–clamped boundary conditions, respectively. The maximum error value for different circumferential mode decreases as n increases. For long shells with the two boundary conditions, the error is always large for $n = 1$. Considering the clamped–clamped boundary conditions, the error is below 10 percent in the range of $L/R > 7.2$ for $n = 2$; and in the range of $L/R > 4$ for $n = 3$; and in the range of $L/R > 2.4$ for $n = 4$; and in the range of $L/R > 1.6$ for $n = 5$.

The effects of stiffness of stiffener and stiffening type on the frequencies error are shown in Figs. 9 and 10, respectively. Fig. 9 illustrates frequencies comparison of stiffened shell with a stiffener cross-section higher of 0.582 cm; the stiffness of ring becomes large as the height increases. Fig. 10 shows the relative error with C–C boundary conditions for different stiffening types which are external, internal and symmetrical, respectively. Here the symmetrical is introduced to make a comparison. The eccentricity of the centroid of ring stiffener $e_2$ equals to zero as the cross-section of ring is symmetrical. As the circumferential number $n$ increases, the errors decrease for these three kinds of stiffening type.

## 4. Conclusions

The wave propagation approach is used to analyze the free vibration of ring-stiffened cylindrical shell under initial hydrostatic pressure, based on Flügge classical thin shell theory and orthotropic method in this paper. The accuracy and validity of the wave propagation approach is studied, through comparison for frequencies with those of exact solution. The conclusions are obtained from analysis above.

The wave propagation approach is accurate for calculation of frequency of ring-stiffened cylindrical shell for SD–SD boundary conditions, both the analytical and numerical methods prove that the wave propagation approach is absolutely equal to the traditional method. For those other than SD–SD boundary conditions, some errors will be introduced due to neglecting the coupling effects between axial and circumferential modes. The wave propagation method has high accuracy for longer shell and large circumferential number $n$. The effect of initial stress makes the frequency error larger for some certain lower circumferential modes.

## Appendix A. Forces and moments

Eight initial forces including membrane forces $N_x$, $N_\theta$, $N_{x\theta}$ and $N_{x\theta}$, bending moments $M_x$ and $M_\theta$, torsioning moments $M_{x\theta}$ and $M_{\theta x}$ are given

$$N_x = B\left(\frac{\partial u}{\partial x} + \upsilon\frac{\partial v}{R\partial\theta}\right) - B\upsilon\frac{w}{R} + \frac{D}{R}\frac{\partial^2 w}{\partial x^2}$$

$$N_\theta = B\left[(1+\mu_2)\left(\frac{\partial v}{R\partial\theta} - \frac{w}{R}\right) + \upsilon\frac{\partial u}{\partial x} - \chi_2\left(\frac{w}{R} + \frac{\partial^2 w}{R\partial\theta^2}\right)\right] - \frac{D}{R}\left(\frac{\partial^2 w}{R^2\partial\theta^2} + \frac{w}{R^2}\right)$$

$$N_{\theta x} = \frac{1-\upsilon}{2}B\left(\frac{\partial u}{R\partial\theta} + \frac{\partial v}{\partial x}\right) + \frac{D}{R}\frac{1-\upsilon}{2}\left(\frac{\partial u}{R^2\partial\theta} - \frac{\partial^2 w}{R\partial x\partial\theta}\right)$$

$$N_{x\theta} = \frac{1-\upsilon}{2}B\left(\frac{\partial u}{R\partial\theta} + \frac{\partial v}{\partial x}\right) + \frac{D}{R}\frac{1-\upsilon}{2}\left(\frac{\partial v}{R\partial x} + \frac{\partial^2 w}{R\partial x\partial\theta}\right)$$

$$M_\theta = D\left[-(1+\eta_2)\left(\frac{w}{R^2} + \frac{\partial^2 w}{R^2\partial\theta^2}\right) - \upsilon\frac{\partial^2 w}{\partial x^2} + \zeta_2\left(\frac{\partial v}{R^2\partial\theta} - \frac{w}{R^2}\right)\right]$$

$$M_x = D\left[-\frac{\partial^2 w}{\partial x^2} - \upsilon\frac{\partial^2 w}{R^2\partial\theta^2} - \frac{\partial u}{R\partial x} - \upsilon\frac{\partial v}{R^2\partial\theta}\right]$$

$$M_{x\theta} = D\left[(1-\upsilon)\left(-\frac{\partial^2 w}{R\partial x\partial\theta} - \frac{\partial v}{R\partial x}\right)\right]$$

$$M_{\theta x} = D\left[(1-\upsilon)\left(-\frac{\partial^2 w}{R\partial x\partial\theta} + \frac{1}{2}\frac{\partial u}{R^2\partial\theta} - \frac{1}{2}\frac{\partial v}{R\partial x}\right) - \eta_{t_2}\frac{\partial^2 w}{R\partial x\partial\theta}\right]$$

where $\mu_2 = EA_2/Bd_2$, $\chi_2 = EA_2e_2/Rd_2B$, $\eta_2 = EI_2/Dd_2$, $\eta_{t_2} = GJ_2/Dd_2$, $\zeta_2 = \chi_2(12R^2/h^2)$.

## Appendix B. The coefficients in the matrix of Eq. (3)

$$K_{11} = k_m^2R^2 + \frac{1-\upsilon}{2}(1+k)n^2 - \frac{QR}{B}\left(n^2 + \frac{1}{2}k_m^2R^2\right)$$

$$K_{12} = -\frac{1+\upsilon}{2}nk_mR$$

$$K_{13} = \upsilon k_mR + kk_m^3R^3 - \frac{1-\upsilon}{2}kn^2k_mR + \frac{QR}{B}k_mR$$

$$K_{21} = \frac{1+\upsilon}{2}nk_mR$$

$$K_{22} = (1+\mu_2-\zeta_2k)n^2 + \frac{1-\upsilon}{2}(1+3k)k_m^2R^2 - \frac{QR}{B}\left(n^2 + \frac{1}{2}k_m^2R^2\right)$$

$$K_{23} = n(1+\mu_2-\eta_2k) + \frac{3-\upsilon}{2}knk_m^2R^2 + (\eta_2-\zeta_2)kn^3 - \frac{QR}{B}n$$

$$K_{31} = -\upsilon k_mR - kk_m^3R^3 + \frac{1-\upsilon}{2}kn^2k_mR - \frac{QR}{B}k_mR$$

$$K_{32} = n(1+\mu_2) + k\frac{3-\upsilon}{2}nk_m^2R^2 - \zeta_2kn^3 - \frac{QR}{B}n$$

$$K_{33} = (1+\mu_2) + k[k_m^4R^4 + (2+\eta_{t_2})n^2k_m^2R^2 + (1+\eta_2)n^4 + (1+\zeta_2) - (2+\eta_2+2\zeta_2)n^2] - \frac{QR}{B}\left(n^2 + \frac{1}{2}k_m^2R^2\right)$$

## Appendix C. The coefficients of Eq. (6)

$$a_1 = -\frac{1}{\gamma}(K_{11}+K_{22}+K_{33})$$

$$a_2 = \frac{1}{\gamma^2}(K_{11}K_{22}+K_{22}K_{33}+K_{11}K_{33}-K_{13}^2-K_{23}K_{32}-K_{12}^2)$$

$$a_3 = \frac{1}{\gamma^3}(-K_{11}K_{22}K_{33}-K_{32}K_{21}K_{13}-K_{12}K_{23}K_{31}+K_{13}^2K_{22}+K_{11}K_{23}K_{32}+K_{12}^2K_{33})$$

## Appendix D. The coefficients of Eq. (8)

$$g_8 = k\left(k-1+\frac{1}{2}\frac{QR}{B}\right)\left(\frac{1-\upsilon}{2}(1+3k)-\frac{1}{2}\frac{QR}{B}\right)R^8$$

$$\begin{aligned}
g_6 = & -k\left(\frac{1-\upsilon}{2}(1+3k)d_1-\frac{1}{2}\frac{QR}{B}(d_1+d_2)+d_2\right)R^6+(3-\upsilon)\frac{1+\upsilon}{2}k^2n^2R^6\\
& +\left(1-\frac{1}{2}\frac{QR}{B}\right)\left(\frac{1-\upsilon}{2}(1+3k)-\frac{1}{2}\frac{QR}{B}\right)\left(k(2+\eta_{t_2})n^2-\frac{1}{2}\frac{QR}{B}\right)R^6-\left(\frac{3-\upsilon}{2}\right)^2\left(1-\frac{1}{2}\frac{QR}{B}\right)k^2n^2R^6\\
& -k\left(\upsilon-k\frac{1-\upsilon}{2}n^2+\frac{QR}{B}\right)\left((1-\upsilon)(1+3k)-\frac{QR}{B}\right)R^6+k^2d_2R^6-k\left(\frac{1+\upsilon}{2}\right)^2n^2R^6\\
g_4 = & \left(\frac{1-\upsilon}{2}(1+3k)d_1-\frac{1}{2}\frac{QR}{B}(d_1+d_2)+d_2\right)\left(k(2+\eta_{t_2})n^2-\frac{1}{2}\frac{QR}{B}\right)R^4-\frac{1+\upsilon}{2}(d_3+d_4)knR^4\\
& +d_5\left(1-\frac{1}{2}\frac{QR}{B}\right)\left(\frac{1-\upsilon}{2}(1+3k)-\frac{1}{2}\frac{QR}{B}\right)R^4-2kd_2\left(\upsilon-k\frac{1-\upsilon}{2}n^2+\frac{QR}{B}\right)R^4-k^2\left(\frac{3-\upsilon}{2}\right)^2d_1n^2R^4\\
& -(3-\upsilon)\frac{1+\upsilon}{2}\left(\upsilon-k\frac{1-\upsilon}{2}n^2+\frac{QR}{B}\right)kn^2R^4+\left(\upsilon-k\frac{1-\upsilon}{2}n^2+\frac{QR}{B}\right)^2\left(\frac{1-\upsilon}{2}(1+3k)-\frac{1}{2}\frac{QR}{B}\right)R^4\\
& +k\frac{3-\upsilon}{2}\left(1-\frac{1}{2}\frac{QR}{B}\right)(d_4+d_3)nR^4-d_1d_2kR^4+\left(\frac{1+\upsilon}{2}\right)^2\left(k(2+\eta_{t_2})n^2-\frac{1}{2}\frac{QR}{B}\right)n^2R^4\lambda^4\\
g_2 = & d_1d_2\left(k(2+\eta_{t_2})n^2-\frac{1}{2}\frac{QR}{B}\right)R^2+d_5\left(\frac{1-\upsilon}{2}(1+3k)d_1-\frac{1}{2}\frac{QR}{B}(d_1+d_2)+d_2\right)R^2\\
& +\frac{1+\upsilon}{2}\left(\upsilon-k\frac{1-\upsilon}{2}n^2+\frac{QR}{B}\right)(d_3+d_4)nR^2+d_2\left(\upsilon-k\frac{1-\upsilon}{2}n^2+\frac{QR}{B}\right)^2R^2\\
& +k\frac{3-\upsilon}{2}d_1(d_4+d_3)nR^2-\left(1-\frac{1}{2}\frac{QR}{B}\right)d_3d_4R^2+d_5\left(\frac{1+\upsilon}{2}\right)^2n^2R^2\lambda^2\\
g_0 = & d_1d_2d_5-d_1d_3d_4
\end{aligned}$$

where

$$d_1 = \gamma\omega^2-\frac{1-\upsilon}{2}(1+k)n^2+\frac{QR}{B}n^2 \quad d_2 = \gamma\omega^2-(1+\mu_2)n^2+\zeta_2kn^2+\frac{QR}{B}n^2$$

$$d_3 = (1+\mu_2)n-\zeta_2kn^3-\frac{QR}{B}n, \quad d_4 = -\zeta_2kn^3+\eta_2(-n+n^3)k+(1+\mu_2)n-\frac{QR}{B}n$$

$$d_5 = -k(1+\eta_2)n^4+k(2+\eta_2+2\zeta_2)n^2-k(1+\zeta_2)-(1+\mu_2)+\frac{QR}{B}n^2+\gamma\omega^2$$

## Appendix E. The coefficients in the matrix of Eq. (17)

$$K'_{11} = m^2\beta^2+\frac{1-\nu}{2}(1+k)n^2-\frac{QR}{B}\left(n^2+\frac{m^2\beta^2}{2}\right)$$

$$K'_{12} = \frac{1+\nu}{2}mn\beta$$

$$K'_{13} = -\nu m\beta-km^3\beta^3+\frac{1-\nu}{2}kmn^2\beta-\frac{QR}{B}m\beta$$

$$K'_{21} = \frac{1+v}{2}mn\beta$$

$$K'_{22} = (1+\mu_2)n^2 + \frac{1-v}{2}(1+3k)m^2\beta^2 - \zeta_2 kn^2 - \frac{QR}{B}\left(n^2 + \frac{m^2\beta^2}{2}\right)$$

$$K'_{23} = [(1+\mu_2) - k\eta_2]n + (\eta_2 - \zeta_2)n^3 k + \frac{3-v}{2}m^2 n\beta^2 k - \frac{QR}{B}n$$

$$K'_{31} = -vm\beta - km^3\beta^3 + \frac{1-v}{2}kmn^2\beta - \frac{QR}{B}m\beta$$

$$K'_{32} = (1+\mu_2)n + \frac{3-\upsilon}{2}m^2 n\beta^2 k - \zeta_2 n^3 k - \frac{QR}{B}n$$

$$\begin{aligned} K'_{33} = & -k[-m^4\beta^4 - (2+\eta_{t_2})m^2n^2\beta^2 - (1+\eta_2)n^4 + (2+\eta_2+2\zeta_2)n^2 - (1+\zeta_2)] \\ & - \frac{QR}{B}\left(n^2 + \frac{m^2\beta^2}{2}\right) + (1+\mu_2) \quad (2-28) \end{aligned}$$

where $\beta = \frac{\pi R}{L}$.

## Appendix F. The coefficients of Eq. (18)

$$b_1 = -\frac{1}{\gamma}(K'_{11} + K'_{22} + K'_{33})$$

$$b_2 = \frac{1}{\gamma^2}(K'_{11}K'_{22} + K'_{11}K'_{33} + K'_{22}K'_{33} - K'^2_{13} - K'^2_{12} - K'_{23}K'_{32})$$

$$\begin{aligned} b_3 = & \frac{1}{\gamma^3}(K'_{11}K'_{23}K'_{32} + K'_{22}K'_{13} + K'_{33}K'_{12} + K'_{12}K'_{13}(K'_{23} + K'_{32}) \\ & - K'_{11}K'_{22}K'_{33}) \end{aligned}$$

## References


[1] W. Flügge, *Stress in Shells*, second ed., Springer, Berlin, 1973.
[2] R.N. Arnold, G.B. Warburton, Flexural vibrations of the walls of thin cylindrical shells having freely supported ends, *Proceedings of the Royal Society A* 197 (1949) 238–256.
[3] R.N. Arnold, G.B. Warburton, The flexural vibrations of thin cylinders, *Proceedings of the Institution of Mechanical Engineers A* 167 (1953) 62–80.
[4] C.B. Sharma, Calculation of natural frequencies of fixed-free circular cylindrical shells, *Journal of Sound and Vibration* 35 (1974) 55–76.
[5] A.W. Leissa, Vibration of Shells, NASA, SP-288, 1973.
[6] K. Forsberg, Influence of boundary conditions on the modal characteristics of thin cylindrical shells, *AIAA Journal* 2 (1964) 2150–2157.
[7] G.B. Warburton, J. Higgs, Natural frequencies of thin cantilever cylindrical shells, *Journal of Sound Vibration* 11 (3) (1970) 335–338.
[8] G.B. Warburton, Vibrations of thin circular cylindrical shells, *Journal of Mechanical Engineering Science* 7 (4) (1965) 399–407.
[9] R.L. Goldman, Mode shapes and frequencies of clamped–clamped cylindrical shells, *AIAA Journal* 12 (1974) 1755–1756.
[10] A. Ludwig, R. Krieg, An analytical quasi-exact method for calculating eigenvibrations of thin circular cylindrical shells, *Journal of Sound and Vibration* 74 (2) (1981) 155–174.
[11] C. Wang, J.C.S. Lai, Prediction of natural frequencies of finite length circular cylindrical shells, *Applied Acoustics* 59 (2000) 385–400.
[12] X.M. Zhang, G.R. Liu, K.Y. Lam, Vibration analysis of thin cylindrical shells using wave propagation approach, *Journal of Sound and Vibration* 239 (3) (2001) 397–403.
[13] X.M. Zhang, G.R. Liu, K.Y. Lam, Coupled vibration analysis of fluid-filled cylindrical shells using the wave propagation approach, *Applied Acoustics* 62 (2001) 229–243.
[14] X.M. Zhang, Frequency analysis of submerged cylindrical shells with wave propagation approach, *International Journal of Mechanical Science* 44 (2004) 1259–1273.
[15] X.M. Zhang, Vibration analysis of cross-ply laminated composite cylindrical shells using the wave propagation approach, *Applied Acoustics* 62 (2001) 1221–1228.
[16] Li. Xuebin, Study on free vibration analysis of circular cylindrical shells using wave propagation, *Journal of Sound and Vibration* 311 (2008) 667–682.
[17] M.B. Xu, X.M. Zhang, Vibration power flow in a fluid-filled cylindrical shell, *Journal of Sound and Vibration* 218 (4) (1998) 587–598.
[18] M.B. Xu, X.M. Zhang, W.H. Zhang, Space-harmonic analysis of input power flow in a periodically stiffened shell filled with fluid, *Journal of Sound and Vibration* 222 (4) (1999) 531–546.
[19] M.B. Xu, X.M. Zhang, W.H. Zhang, The effect of wall joint on the vibrational power flow propagation in a fluid-filled shell, *Journal of Sound and Vibration* 224 (3) (1999) 395–410.
[20] M.B. Xu, W.H. Zhang, Vibrational power flow input and transmission in a circular cylindrical shell filled with fluid, *Journal of Sound and Vibration* 243 (4) (2000) 387–403.
[21] N.L. Basdekas, M. Chi, Response of oddly stiffened circular cylindrical shell, *Journal of Sound and Vibration* 17 (2) (1971) 187–206.
[22] G.D. Galletly, On the in-vacuo vibrations of simply supported, ring-stiffened cylindrical shells, *Proceeding of the Second National Congress of Applied Mechanics Processing*, 1954, pp. 225–231.
[23] T. Wah, W.C.L. Hu, Vibration analysis of stiffened cylinders including inter-ring motion, *Journal of Acoustical Society of America* 43 (5) (1968).
[24] G.C. Everstine, Ring-stiffened cylinder, *Proceeding of NSRDC-NASTRAN Colloquium*, 1970.

[25] A.A. Jafari, M. Bagheri, Free vibration of non-uniformly ring stiffened cylindrical shells using analytical, experimental and numerical methods, *Thin-Walled Structures* 44 (2006) 82–90.
[26] B. Mustafa, R. Ali, An energy method for free vibration analysis of stiffened circular cylindrical shells, *Composite Structures* 32 (2) (1989) 335–363.
[27] W.H. Hoppmann, Some characteristics of the flexural vibrations of orthogonally stiffened cylindrical shells, *Journal of Acoustical Society of America* 30 (1958) 77–82.